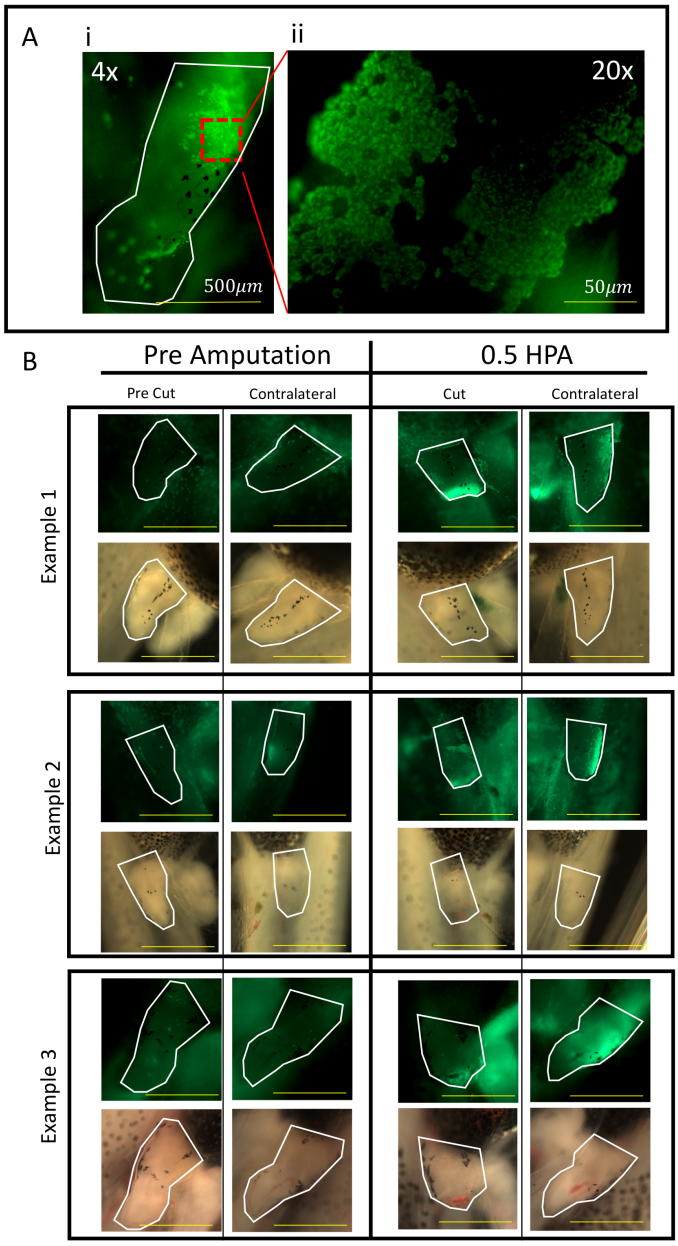

Supplementary Fig. 1. Examples of contralateral DiBAC$_4$(3) staining.

Examples 1 (from Figure 3C), 2, and 3 represent multiple iterations of what the staining on the cut and contralateral limbs looks like before and after amputation. In order to better describe the signal pattern, higher magnitude (20x) images were taken of contralateral limbs soaked in DiBAC$_4$(3) before amputation and 0.5 HPA (**Ai**). The limb was removed and placed on a depression slide for imaging at 20x (**Aii**). Three samples of froglets (in bright field and DiBAC$_4$(3)) shown immediately before amputation, and 0.5 HPA (**B**). Scale bar 500 μm.

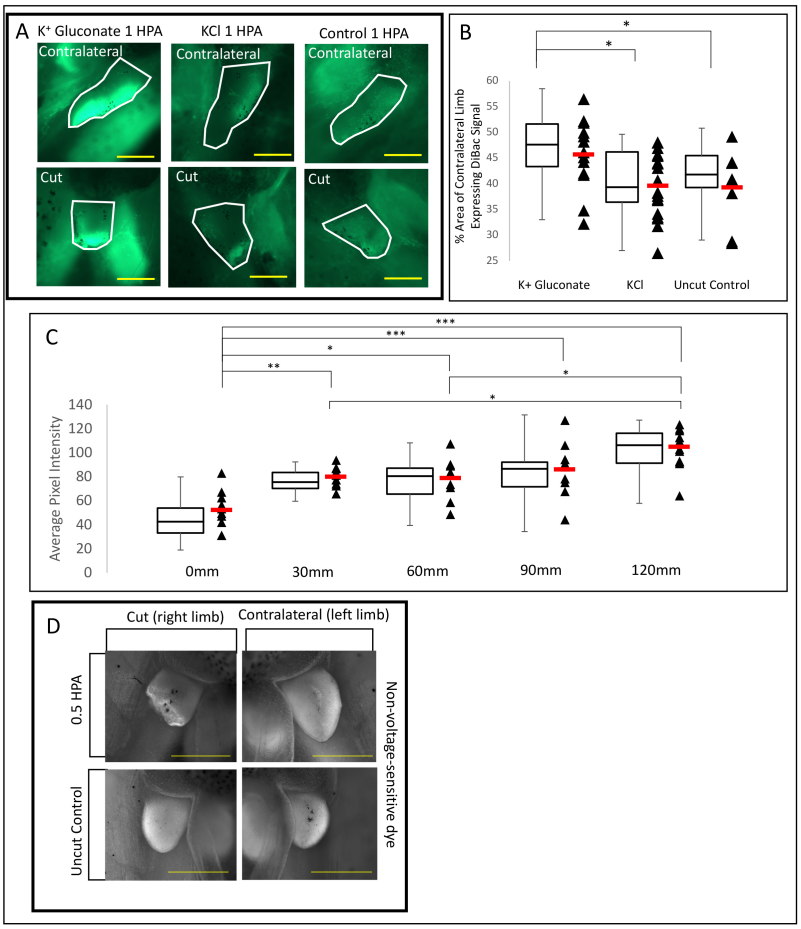

Supplementary Fig. 2. Validating dye imaging of depolarization in froglet legs.

To validate that $DiBAC_4(3)$ is detecting membrane voltage changes towards a less negative value, froglets were amputated and then soaked in $DiBAC_4(3)$ and either potassium gluconate (to depolarize cells) or potassium chloride. Limbs are outlined in white. Animals soaked in a 90mM solution of potassium (potassium gluconate) following amputation exhibited significantly more intense $DiBAC_4(3)$ signal (**A**) than *a)* untreated animals and *b)* animals that were soaked in 90mM solution containing depolarizing potassium and hyperpolarizing chloride (KCl). These data suggest that $DiBAC_4(3)$ illuminates positively charged cells and that the fluorescent cells in the contralateral limb responding to amputation are depolarized (ANOVA, KCl n=20, potassium gluconate n=15, control n=12, $p<0.01$). The experiment was replicated three times (**B**). Dose dependence of fluorescent dye signal on external K^+ level was observed: unamputated froglets treated with 0 mM, 30 mM, 60 mM, 90 mM, and 120 mM potassium gluconate were imaged, and the signal limb image intensity was quantified. Increased potassium gluconate concentration increased signal intensity on the limbs such that there was a significant difference ($p\leq0.01$) between 0 mM (n=9), and 30 mM (n=9), 60 mM (n=8), 90 mM (n=9), and 120 mM (n=11) potassium gluconate. There was also a significant difference between 30 mM and 120 mM potassium gluconate ($p<0.01$), and between 60 mM and 120 mM potassium gluconate ($p<0.01$). The experiment was replicated three times (**C**). 10 μM Acridine orange was used to stain limbs of both amputated and amputated froglets at 1 HPA. Froglets were amputated and then allowed to soak in the acridine orange and 0.1X MMR for 60 minutes. There was no detectable difference in intensity between contralateral limbs of uncut and cut froglets (n=12 cut, n=18 uncut). The experiment was replicated twice (**D**). Scale bar 500 μm.

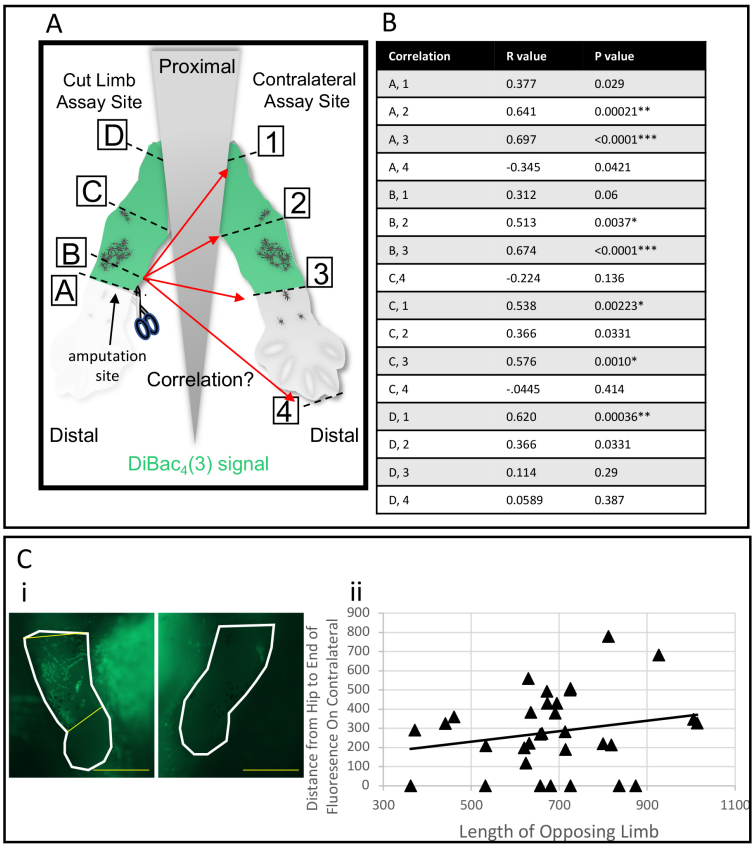

Correlation	R value	P value
A, 1	0.377	0.029
A, 2	0.641	0.00021**
A, 3	0.697	<0.0001***
A, 4	-0.345	0.0421
B, 1	0.312	0.06
B, 2	0.513	0.0037*
B, 3	0.674	<0.0001***
C,4	-0.224	0.136
C, 1	0.538	0.00223*
C, 2	0.366	0.0331
C, 3	0.576	0.0010*
C, 4	-.0445	0.414
D, 1	0.620	0.00036**
D, 2	0.366	0.0331
D, 3	0.114	0.29
D, 4	0.0589	0.387

Supplementary Fig. 3. Quantifying spatial correlation between amputation site and contralateral DiBAC$_4$(3) signal.

Regenerative limbs were amputated at a proximal or distal position, and several measurements were made in order to determine if the point of this cut correlated to the area of depolarization on the contralateral (**A**). We produced correlations between positions A, B, C, or D, and 1, 2, 3, or 4. Position A represents the length from the hip to the stump remaining after amputation. Position B represents the distance from the hip joint to the end point of depolarization in the cut limb (which in some cases is the same value as position A). Position C measures the distance from the hip to the midpoint of depolarization on the amputated limb. Position D measures from the hip to the start point of depolarization on the amputated limb. Position 1 measures from the hip to the start point of depolarization on the contralateral limb. Position 2 measures the distance from the hip to the midpoint of depolarization on the contralateral limb. Position 3 measures from the hip to the end point of depolarization on the contralateral limb. Position 4 measures the entire length of the contralateral limb (A). Regressions from each of these correlations resulted in significant relationships between several positions **(B).** To determine whether the signal observed in the limb of froglets that underwent spinal cord transections was "mirroring" information about the length of the opposing limb, we performed a correlation regression on the length of the limb and the length that the DiBAC$_4$(3) signal extended down the opposing limb in order to determine if there was a spatial relationship **(Ci).** The correlation suggests that the length of the limb and the distance that depolarization extends down the opposing limb are not correlated (Linear Regression Test, n=30, r=0.21, p=0.38) **(Cii)**. Scale bar 500 μm.

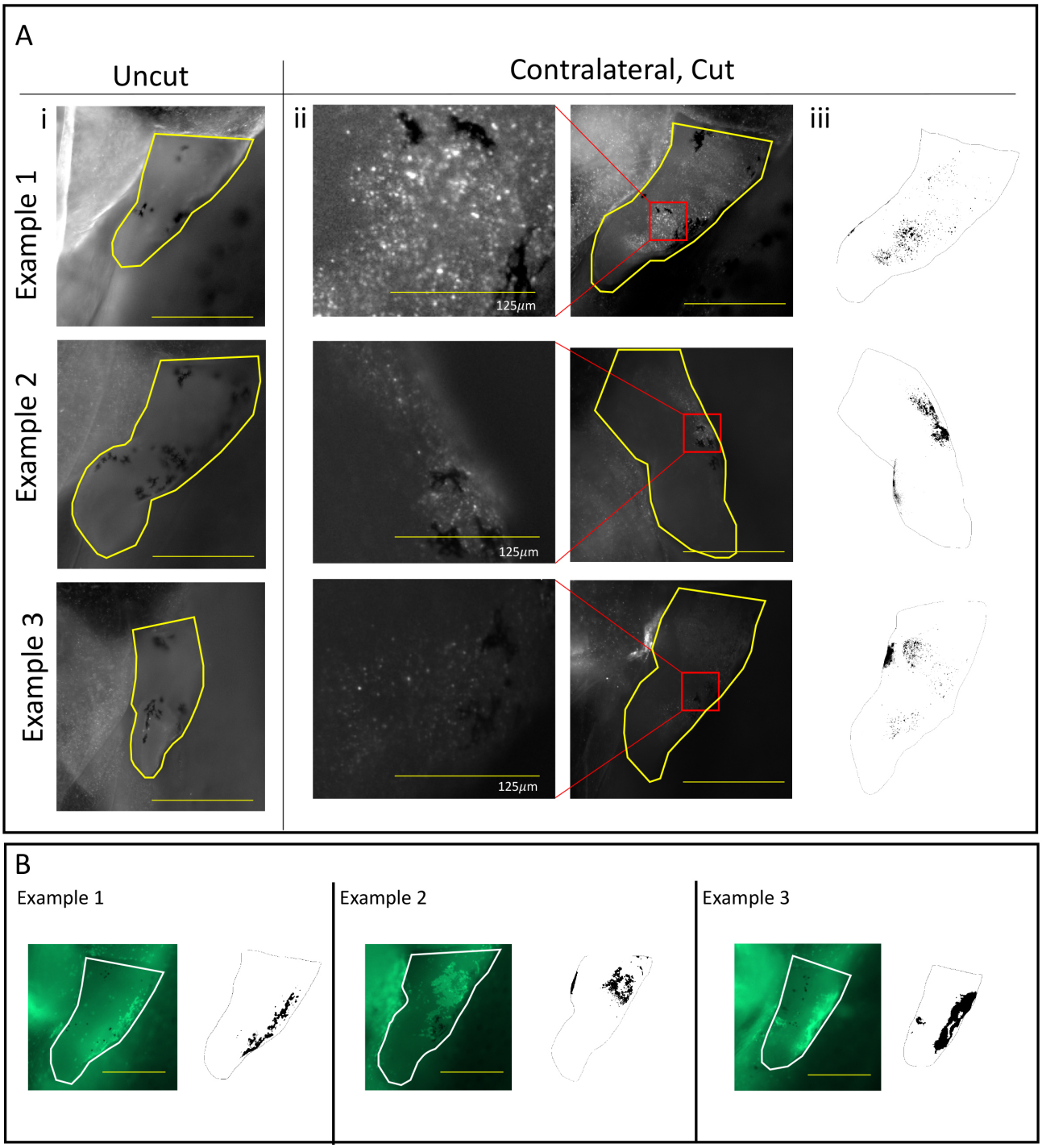

Supplementary Fig. 4. Immunohistochemistry with antibody to Activated Caspase 3 shows pattern of programmed cell death in contralateral limb.

To further characterize cell types involved in BIM, we performed immunohistochemistry with a caspase-3 apoptosis marker for cell death on froglets that had been amputated, allowed to recover for 0.5 hours, and then sacrificed and fixed in MEMFA. Limbs of control froglets that had not been amputated little to no observable cells positive for CC3 activity (n=12) **(Ai).** Contralateral limbs of amputated froglets showed CC3 positive regions (n=12) **(Aii).** Pattern and distribution of CC3 positive cells was similar but not the same as the patterns observed froglet limbs stained with $DiBAC_4(3)$ (**Aiii-B**).

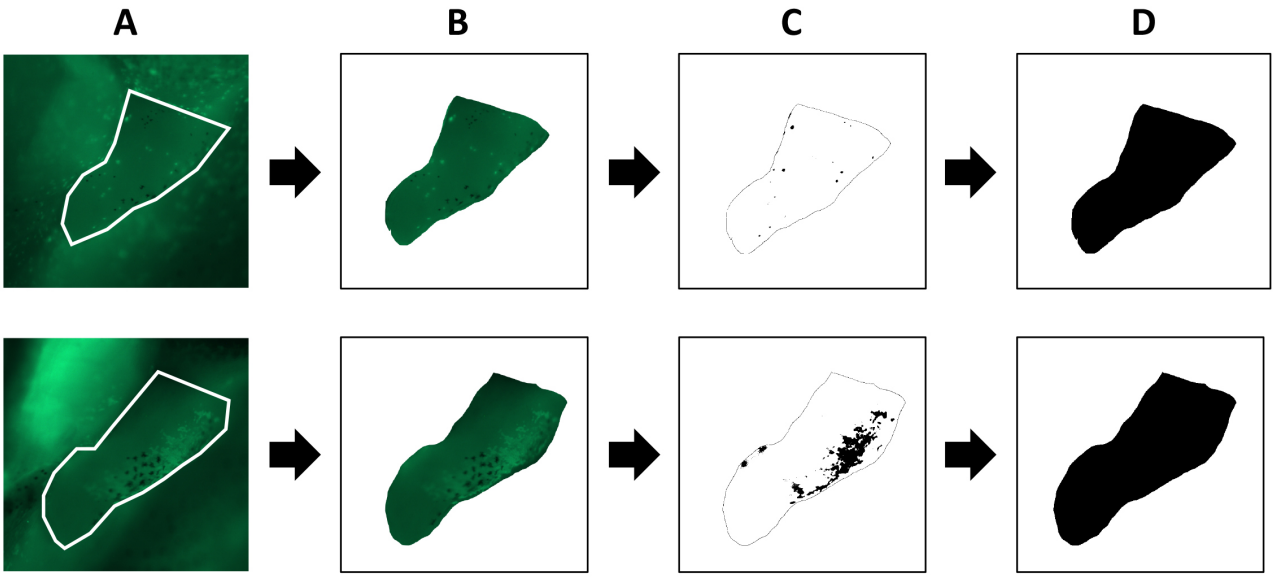

Supplementary Fig. 5. Work-flow for the quantitative image analysis of froglet limbs using Photoshop and ImageJ.

Quantitative image analysis was performed by taking raw images **(A)** and using the lasso tool in Photoshop to trace the anatomy of the limb; then the image background was removed **(B)**. This process was completed for all images in a given imaging session, and the images from that session imported as a stack into imageJ. We used a binary thresholding approach to avoid having to make any assumptions about a linear correlation between dye intensity and V_{mem}. The color thresholding tool in imageJ was used on an image exhibiting an average amount of signal in the limb and background for the stack of images. The threshold was set such that the amount of signal clearly visible to the human eye on the limb was present in the binary image **(C)**. This same threshold value was then applied to all of the images in the stack, and the total pixel area (total area of $DiBAC_4(3)$ measured. The same image stack was then thresholded again, this time such that the entirety of the limb was covered with black pixels, and the area (the entire area of the limb) was measured **(D)**. The area value acquired in **C** was divided by the area value in **D** to yield a ratio of area signal to total area of limb. Each imaging session contained both controls and cut animals to prevent any possible inconsistencies arising from batch to batch variability in dye preparation.